NASA TECHNICAL NOTE

NASA TN D-2955

NASA TN D-2955

SHOCK-TUBE GAS TEMPERATURE MEASUREMENTS BY INFRARED MONOCHROMATIC RADIATION PYROMETRY

by Milton R. Lauver, Jerry L. Hall, and Frank E. Belles

Lewis Research Center
Cleveland, Ohio

NATIONAL AERONAUTICS AND SPACE ADMINISTRATION • WASHINGTON, D. C. • AUGUST 1965

SHOCK-TUBE GAS TEMPERATURE MEASUREMENTS BY INFRARED MONOCHROMATIC RADIATION PYROMETRY

By Milton R. Lauver, Jerry L. Hall, and Frank E. Belles

Lewis Research Center
Cleveland, Ohio

NATIONAL AERONAUTICS AND SPACE ADMINISTRATION

For sale by the Clearinghouse for Federal Scientific and Technical Information
Springfield, Virginia 22151 – Price $1.00

SHOCK-TUBE GAS TEMPERATURE MEASUREMENTS BY INFRARED MONOCHROMATIC RADIATION PYROMETRY

by Milton R. Lauver, Jerry L. Hall, and Frank E. Belles

Lewis Research Center

SUMMARY

Gas temperature histories in a shock tube were determined by an infrared monochromatic radiation pyrometer technique. A 10 percent carbon dioxide-argon mixture was studied with both incident and reflected shocks. Measured temperatures of 1100° to 3300° K immediately behind the incident shocks were in good agreement with the temperatures calculated by one-dimensional wave theory from the shock velocity. Measured temperatures of 1900° to 3550° K behind reflected shocks were in good agreement for short reflection distances with those calculated by one-dimensional wave theory from the incident shock velocity. The relation between the velocity attenuations and the temperature and pressure rises behind incident shocks was in general agreement with strong shock theory. The change in gas temperature with time behind a reflected shock was adequately calculated from the dissociation rate of carbon dioxide and the measured pressure history of the gas mixture.

INTRODUCTION

The shock tube has one of its prime applications in the study of high-temperature rate processes in gases. Commonly, these processes have a strong temperature dependence, and it is therefore necessary to know the temperature of the experiment quite accurately. This need can be met nicely so long as incident shock waves are used to heat the gas, because one-dimensional theory, plus the thermodynamic properties of the gas, can be used to calculate the shocked gas temperature from the measured velocity of the wave. Very often, however, it is convenient or even necessary to study processes behind reflected shocks, in order to take advantage of the higher temperatures and pressures that can be produced without unduly straining the capacities of conventional shock tubes. In that event, it is no longer so clear that the temperature can be calculated accurately; interactions of the reflected shock with the boundary layer (ref. 1) and with the pressure gradient created by attenuation of the incident shock (ref. 2) introduce complications.

This problem has been widely recognized, and measurements of reflected gas temperature have recently appeared in the literature. For the most part they

were made by the line-reversal method (refs. 3 and 4), although in one case the rate of a chemical reaction was used as an indication of temperature (ref. 5). The purpose of the present work was to study reflected shock temperatures by a more direct method based on simultaneous measurements of infrared spectral radiance and emissivity. Among the advantages of the infrared method are the following: (1) there is no need to introduce sodium salts or other sources of emission; (2) good time resolution is possible; and (3) a very wide temperature range can be covered, a range not limited by the available brightness temperature of a light source as it is in the reversal method.

This report gives temperatures measured behind reflected shocks in a gas that is typical of mixtures likely to be used in chemical studies, 10 percent carbon dioxide-90 percent argon. The temperature range was 1900° to 3550° K. A series of temperatures measured at 50 to 200 microseconds after the reflected wave passed the observation station were extrapolated to zero time and compared with values calculated from the velocity of the incident wave. Two detailed temperature-time records are also presented; these show the effects of shock attenuation on both the incident and the reflected shock temperature.

APPARATUS AND EXPERIMENTAL PROCEDURE

Basis of Emission-Absorption Pyrometry

The infrared monochromatic radiation (IMRA) method of gas temperature measurement has been described elsewhere (refs. 6 and 7). It is based on the fact that the radiance of a hot gas depends on the gas temperature and on the number of gaseous entities (molecules, free radicals, or atoms) emitting radiation. Consequently, by measuring the absolute intensity of radiation (spectral radiance) and the relative number density of emitters (spectral emissivity), the temperature of a gas can be calculated. Figure 1 shows schematically the information recorded in a shock-tube experiment and the way in which it is reduced to a temperature measurement.

The measurement of spectral emission is straightforward. The infrared detection system response to the hot gas emission V_g (fig. 1) is compared with

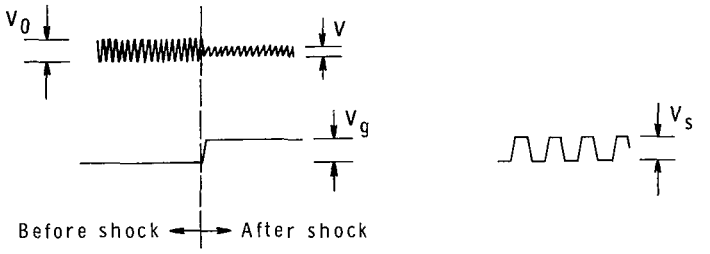

Figure 1. - Basis of infrared monochromatic radiation pyrometer. Emissivity ε = absorbtivity = $1 - (V/V_0)$. Radiance $N_{\lambda, g} = \varepsilon C_1 \lambda^{-5} / (e^{C_2/\lambda T_g} - 1)$.

its response to a calibrated standard infrared source V_s and converted to absolute units by means of calibration factors. The result is a spectral radiance $N_{\lambda,g}$ in terms of watts steradian^{-1} centimeter^{-2} micron^{-1} at a specific wavelength. The effect of the number of emitters is accounted for by absorption spectroscopy at the same wavelength. The reduction in radiance of a chopped transmitted light beam from V_0 to V volts determines the spectral absorptivity $(1 - V/V_0)$, which is equal to the spectral emissivity ϵ.

Kirchoff's radiation law relates the spectral radiance of a hot gas to that of an ideal blackbody radiator. Planck's law relates the spectral radiance of an ideal blackbody radiator to its temperature and emissivity. Combining these laws results in the following relation between the spectral radiance of a gas $N_{\lambda,g}$, its temperature T_g, and its spectral emissivity ϵ:

$$N_{\lambda,g} = \frac{\epsilon C_1 \lambda^{-5}}{e^{C_2/\lambda T_g} - 1} \tag{1}$$

Thus, inasmuch as C_1 and C_2 are the known Planck radiation constants and $N_{\lambda,g}$ and ϵ are measured at wavelength λ, the gas temperature T_g may be calculated.

Apparatus for Emission-Absorption Pyrometry

A schematic diagram of the shock tube and associated equipment is given in figure 2. A constant intensity of infrared radiation from a glower source

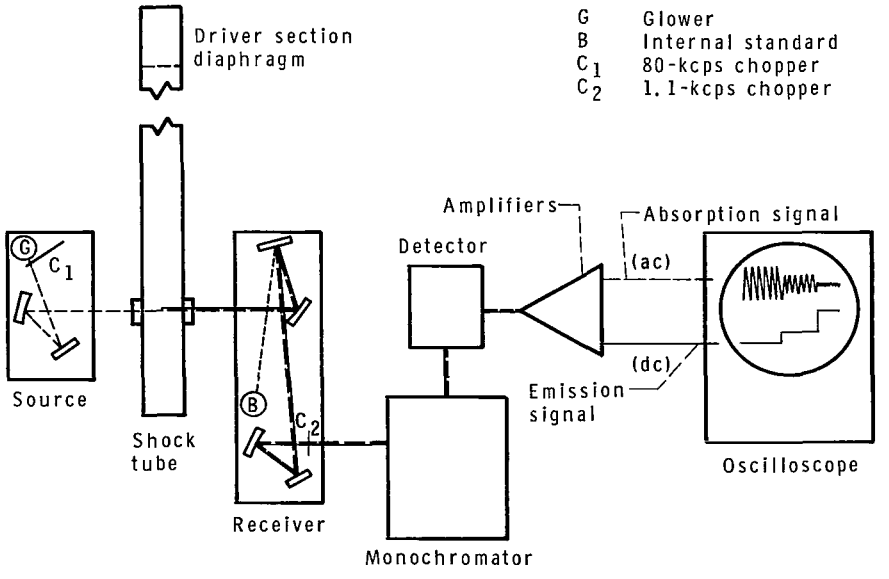

Figure 2. - Schematic diagram of infrared monochromatic radiation pyrometer.

is mechanically chopped at 80 kilocycles per second and sent through the sapphire windows of the shock tube into a prism monochromator and a liquid-nitrogen-cooled indium antimonide detector. The shocked gases emit radiation, which passes out of the shock tube into the same radiation detection system. Its output is amplified by a directly coupled circuit providing a measure of the radiance of the gas (the glower radiance is negligible in comparison to that of the gas). The glower signal is selected by a capacitor-coupled, 80-kilocycle tuned amplifier of high gain. With these amplifiers, the detection system uses frequency separation to distinguish between the emitted and transmitted light, although both are presented simultaneously to the one detector, and sends the resulting signals to different oscilloscope beams for recording.

The principle of temperature measurement used in the IMRA technique corresponds to that of the "Two-Path Method with Comparison Source" (ref. 8). An error analysis by Warshawsky (ref. 9) shows large errors for the latter as the gas temperature rises above the glower temperature. The crucial feature of the IMRA apparatus, which minimizes these errors, consists of chopping the glower radiation before it passes through the test gas. This permits the emitted and transmitted components of the radiation to be separated so that each may be amplified independently by the amount required to obtain easily measurable oscillograms. Without chopping, the light from a source that is emitting more weakly than the gas would be swamped by the gas emission.

Calibration of Pyrometer

The IMRA apparatus was calibrated by determining the transmittance of the shock-tube window and the absolute radiance of the internal secondary-standard source (B in fig. 2), which was a tungsten-ribbon lamp.

The window was found to pass 82 percent of 4.5-microns radiation falling on it. This was the wavelength used for the temperature measurements. Although the center of the asymmetric stretching band of carbon dioxide is at 4.3 microns, the longer wavelength is much more desirable. At 4.5 microns, only the hot gas in the shock tube absorbs light, while the cool carbon dioxide in the room and in the shock-tube boundary layer is almost completely transparent.

The internal standard was compared with a source that had been calibrated at the Bureau of Standards. It was found to emit 2.47 watts steradian^{-1} centimeter^{-2} micron^{-1} at 2.2 microns. The relative sensitivity of the optical system and detector at 4.5 and 2.2 microns was then determined by measuring the radiation from a blackbody source of known temperature at the two wavelengths.

With the foregoing calibration factors at hand, the absolute spectral radiance $N_{\lambda,g}$ of the hot gas at 4.5 microns is readily determined from the following formula:

$$N_{\lambda,g} = \frac{V_g}{V_s} \frac{1}{R} \frac{1}{t_w} N_{\lambda,s} \qquad (2)$$

where

V_g amplitude of emission signal (at 4.5 μ), V

V_s amplitude of signal from internal standard source (at 2.2 μ), V

R sensitivity of the system at 4.5 μ relative to that at 2.2 μ

t_w transmittance of shock-tube window at 4.5 μ

$N_{\lambda, s}$ absolute spectral radiance of internal standard at 2.2 μ

This formula is valid provided the amplification and the slit width are the same when both V_g and V_s are recorded. If they are not the same, the appropriate correction terms must be applied.

Shock Tube

The shock tube was of rectangular cross section, 37 by 74 millimeters. Two circular sapphire windows, 28 millimeters in diameter, were flush mounted opposite one another across the longer dimension. The midpoint of the windows was 3.94 meters from the polyester plastic diaphragm that separated this driven section of the shock tube from the driver section. The midpoint of the windows was 179 millimeters from the downstream end wall of the driven section. This distance to the end wall could be reduced to 27 or 78 millimeters by means of close-fitting plugs. The diaphragms were pressure-burst with helium.

Timing, Pressure, and Recording Instrumentation

Four thin-film resistance gages were mounted upstream of the windows, while one was mounted at the same axial position as the centerline of the windows. These gages marked the time of incident (and in some cases, reflected) shock arrival at the five positions, relative to the first, or trigger, position. The signals were displayed on one beam of a dual beam oscilloscope. The other beam displayed the output of a quartz pressure transducer. This transducer was also located at a position corresponding to the centerline of the windows. A second dual-beam oscilloscope was triggered to display absorption and emission levels from the gas as measured by the IMRA apparatus. Timing pulses from a crystal-controlled secondary frequency standard were recorded on all four oscilloscope beams for each run. A calibration signal for the emission level interrupted about 1100 times per second for identification and a calibration signal for the pressure were also recorded each time.

Figure 3 shows the oscillograph records of infrared absorption and emission for a single experiment. The important features of this typical record are: (1) the large changes of transmitted and emitted light upon passage of the shock waves, (2) the relatively noise-free signals; and (3) the quick recovery of the tuned amplifier in the absorption channel from the ringing induced by step changes, which permits meaningful readings to be made starting

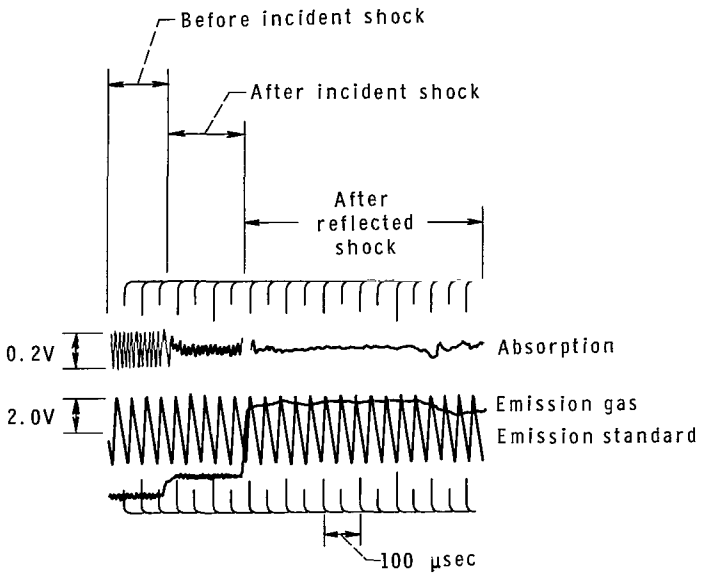

Figure 3. - Typical infrared radiation oscillogram.

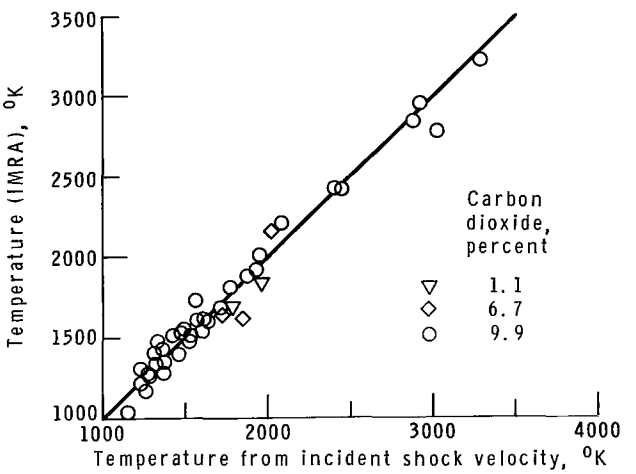

Figure 4. - Comparison of measured and calculated temperatures behind incident shocks in carbon dioxide-argon.

at about 50 microseconds after passage of the shock.

It will be noted in figure 3 that the gas behind the reflected shock in this particular run absorbed almost all of the radiation from the glower source. In many runs of this sort, the portion of the absorption trace after the reflected shock was simultaneously displayed on another oscilloscope at much higher gain, so that the absorptivity could be accurately determined.

Test Gas

A commercially prepared argon-carbon dioxide mixture was used without further treatment. It analyzed 9.9 percent carbon dioxide by volume; the rest was argon. A few tests were made with this gas diluted to 6.7 percent carbon dioxide in argon and with a commercially prepared argon-carbon dioxide mixture that analyzed at 1.1 percent carbon dioxide and the balance, argon.

RESULTS AND DISCUSSION

The results of determinations of gas temperatures behind incident shocks are presented in figure 4, where they are compared with temperatures calculated by simple shock theory from measured shock velocities. The IMRA temperatures were actually measured at several 10-microsecond intervals for each experiment, starting at about 50-microsecond laboratory time when the signals first became readable. Each point in figure 4 was obtained by extrapolating such data back to time zero, the instant when the shock passed the center of the windows. This was done to eliminate effects of shock velocity attenuation on the temperature.

The agreement is good, and as expected, does not seem to be affected by the carbon dioxide concentration over the range studied. Despite this general agreement between measured and calculated incident temperatures, there is

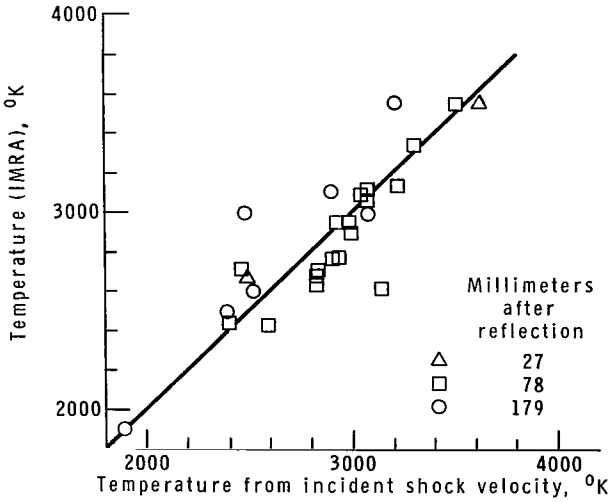

Figure 5. - Comparison of measured and calculated temperatures behind reflected shocks in carbon dioxide-argon.

nevertheless a good deal of scatter evident in figure 4. Part of this scatter is traceable to contamination of the shock-tube windows, but most of it is due to a drifting type of instability of the infrared detector. From run to run, this instability produced uncertainties as large as 10 percent in $N_{\lambda, g}$. Equation (1) shows that this error results in an uncertainty of only about 30° K at temperatures near 1000° K, but the error grows to nearly 300° K at temperatures near 4000° K.

Inasmuch as the main purpose of the work was to measure reflected shock temperatures at levels above 2000° K, it was desirable to reduce the expected scatter in the results as much as possible. This was done by using the incident shock wave as an internal standard for each run. The temperature calculated from the measured shock velocity at the window position, and the measured emissivity of the gas behind the incident wave, were both assumed to be correct. The value of spectral radiance $N_{\lambda, g}$ required to satisfy equation (1) was then calculated. This value, and the measured voltages V_g (incident shock) and V_s, were inserted in equation (2) and used to calculate a lumped instrument factor, $(1/R)(1/t_w)N_{\lambda, s}$.

In each run, then, this individually determined factor was used to convert measured voltages into a series of reflected shock temperatures, starting at about 50 microseconds behind the shock and determined at approximately 10-microsecond intervals. These data were extrapolated to time zero, the instant the reflected shock passed the center of the windows. The resulting measured temperatures are plotted as ordinates in figure 5; the abscissas are the corresponding reflected temperatures graphically (ref. 10) calculated from the velocity of the incident shock as it passed the windows.

Clearly, this means of obtaining calculated reflected shock temperatures for comparison with measured values is rather arbitrary. Its most obvious shortcoming is that it does not allow for the attenuation of the incident wave. However, it is important to see how well the temperatures calculated in this simple way agree with the measured values. Figure 5 shows that they agree quite well, although there are trends in the data. The points obtained with the end wall at its most remote position, 179 millimeters from the windows, tend to be high, and those obtained with the end wall 78 millimeters away tend to be low. This behavior is not inconsistent with that noted in reference 11, which reported that the reflected shock pressure behaved as if the shock decelerated and then accelerated as it receded from the end wall. Despite these trends, the agreement between measured and simply-calculated temperatures is very gratifying. Of the 27 measurements shown in figure 5, 14 are within

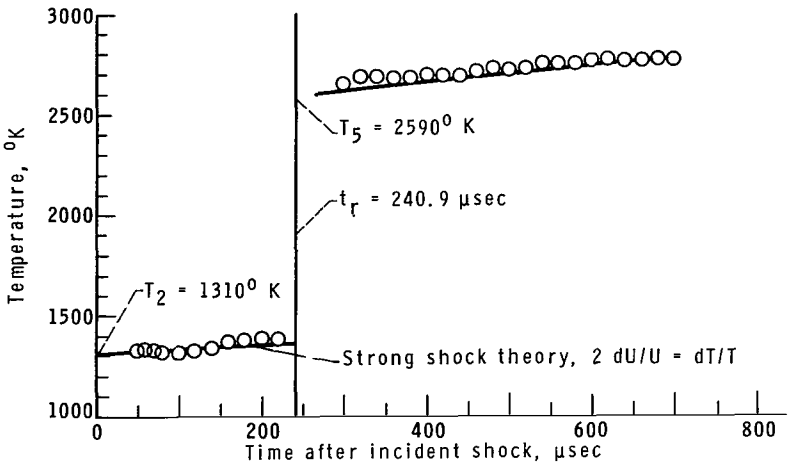

Figure 6. - Experimental and calculated temperatures behind shock waves in carbon dioxide-argon. P_1 = 51.0 torr; incident Mach number, 3.64.

100° K of the line, and only 4 miss it by more than 200° K. It is, however, believed that deviations larger than 100° K are real and that they reflect actual departures of the shocks from ideal one-dimensional behavior.

The two extreme points in figure 5 represent data from oscilloscope records in which the reflected portions could be accurately measured but the incident portions could not. These two points were therefore calculated with the original calibration factors rather than an individually determined factor such as was used for each other point. They are included to extend the temperature range of the reflected data and to indicate that the individual calibration corrections were usually small.

An example of the detail which can be obtained by the IMRA method is given in figure 6, where the temperature history of a shock is followed at 10- to 20-microsecond intervals for 700 microseconds after its passage. Measurement of the incident shock wave velocity U at four successive places just before arrival at the test window showed the velocity to be attenuating at the rate of 1.5×10^{-4} (millimeters per microsecond) per millimeter. Therefore, $dU/U = 1.5\times10^{-4}$ for a 1-microsecond interval. Strong shock theory predicts the relation $2dU/U = dT/T = dP/P$. Therefore, in the first 200 microseconds after the passage of the incident shock, the temperature would be expected to rise from 1310° K (calculated from shock velocity) to about 1388° K and the pressure P from 1.76 to about 1.87 atmospheres. The IMRA measurements showed this rise approximately, as indicated by their conformity to the incident theory line in figure 6. The pressure rose to 1.90 atmospheres, or $dP/P = 3.8\times10^{-4}$; this also shows good agreement with the prediction.

Other observers (ref. 2) have noted a rise in pressure behind reflected shocks. This pressure rise, converted into an isentropic temperature change by the equation $T = T_0(P/P_0)^{[(\gamma-1)/\gamma]}$, where γ is the ratio of specific

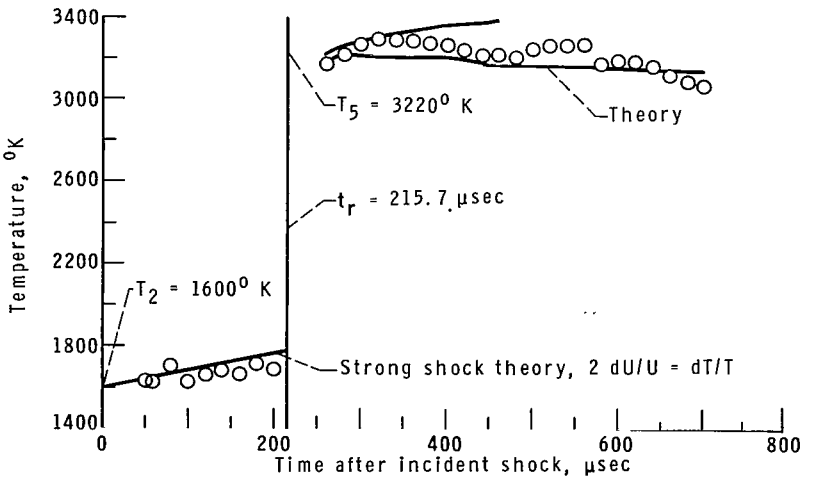

Figure 7. - Experimental and calculated temperatures behind shock waves in carbon dioxide-argon. P_1 = 51.0 torr; incident Mach number, 4.09.

heats and T_o is the reflected shock temperature calculated from incident shock velocity, corresponds very well with the infrared pyrometer results of figure 6.

A second example of detailed analysis is presented in figure 7. Here the temperature following the passage of the reflected shock tends to rise, because of isentropic compression, and tends to decrease because of dissociation according to the equation

$$CO_2 \rightarrow CO + \frac{1}{2} O_2, \quad \Delta H = 65.8 \text{ kilocalories}$$

The reaction has atomic oxygen as an initial product. However, the recombination rate of atomic oxygen is so high at these conditions that this step in the reaction mechanism can be ignored. The following were used to make theoretical temperature calculations: (1) 2.9×10^7 cubic centimeters mole^{-1} second^{-1} for the dissociation rate of carbon dioxide, calculated for 3220° K from the expression given in reference 12, and for the subsequent temperatures after the reflected shock-wave passage, (2) the isentropic temperature corrections from the measured pressures, and (3) negligible back reaction of the carbon monoxide and oxygen to form carbon dioxide. As with the simpler case of figure 6, the agreement of theory and results is gratifying. In this case, figure 7, the attenuation comparisons behind the incident shock are $dU/U = 2.6 \times 10^{-4}$, $dP/P = 4.3 \times 10^{-4}$, and $dT/T = 3.4 \times 10^{-4}$.

CONCLUSIONS

This study of gas temperatures measured in a shock tube by infrared monochromatic radiation pyrometry has led to the following conclusions:

1. Infrared pyrometry of a carbon dioxide-argon gas mixture yielded incident shock temperatures in agreement with those calculated from the incident shock speed by common shock theory, from 1100° to 3300° K.

2. A comparison of reflected shock temperatures measured 27, 78, and 179 millimeters after reflection with temperatures calculated from one-dimensional shock theory shows the latter are generally good for short distances after reflection.

3. Attenuation of the speed of an incident shock wave was accompanied by changes in the gas pressure and temperature in the period following the passage of the shock. The relations between these changes were in general agreement with strong shock theory.

4. The change in gas temperature with time after a reflected shock was adequately calculated from the dissociation rate of carbon dioxide and the pressure history of the gas mixture.

Lewis Research Center,
National Aeronautics and Space Administration,
Cleveland, Ohio, June 4, 1965.

REFERENCES

1. Mark, Herman: The Interaction of a Reflected Shock Wave with the Boundary Layer in a Shock Tube. NACA TM 1418, 1958.

2. Rudinger, George: Effect of Boundary-Layer Growth in a Shock Tube on Shock Reflection from a Closed End. Phys. Fluids, vol 4, no. 12, Dec. 1961, pp. 1463-1473.

3. Napier, D. H.; Nettleton, M.; Simonson, J. R.; and Thackeray, D. P. C.: Temperature Measurement in a Chemical Shock Tube by Sodium-Line Reversal and C_2 Reversal Methods. AIAA J., vol. 2, no. 6, June 1964, pp. 1136-1138.

4. Hurle, I. R.; Russo, A. L.; and Hall, J. Gordon: Spectroscopic Studies of Vibrational Nonequilibrium in Supersonic Nozzle Flows. J. Chem. Phys., vol. 40, no. 8, Apr. 15, 1964, pp. 2076-2089.

5. Johnson, Charles D; and Britton, Doyle: Shock Waves in Chemical Kinetics: The Use of Reflected Shock Waves. J. Chem. Phys., vol. 38, no. 7, Apr. 1, 1963, pp. 1455-1462.

6. Tourin, Richard H.: Monochromatic Radiation Pyrometry of Hot Gases, Plasmas, and Detonations. Temperature - Its Measurement and Control in Science and Industry. Vol. 3, pt. 2, ch. 43, C. M. Herzfeld, ed., Reinhold Publ. Corp., 1962.

7. Tourin, Richard H.; Hecht, Maynard L.; and Dolin, Stanley A.: Measurement of Gas Temperatures in Thermal Pulses by Monochromatic Radiation Pyrometry. Pt. 2 of Measurement of Temperatures in Ionized Gases by Means of Infrared Radiation, Warner & Swasey Co., May 1961, pp. 43-68.

8. Broida, H. P.: Experimental Temperature Measurements in Flames and Hot Gases. Temperature - Its Measurement and Control in Science and Industry. Vol. 2, chap. 17, Hugh C. Wolfe, ed., Reinhold Publ. Corp., 1955.

9. Warshawsky, I.: Measurement of Rocket Exhaust-Gas Temperatures. ISA J., vol. 5, no. 11, Nov. 1958, pp. 91-97.

10. Markstein, George H.: Graphical Computation of Shock and Detonation Waves in Real Gases. ARS J., vol. 29, no. 8, Aug. 1959, pp. 588-590.

11. Brabbs, Theodore A.; Zlatarich, Steven A.; and Belles, Frank E.: Limitations of the Reflected-Shock Technique for Studying Fast Chemical Reactions. J. Chem. Phys., vol. 33, no. 1, July 1960, pp. 307-308.

12. Brabbs, Theodore A; Belles, Frank E; and Zlatarich, Steven A.: Shock-Tube Study of Carbon Dioxide Dissociation Rate. J. Chem. Phys., vol. 38, no. 8, Apr. 15, 1963, pp. 1939-1944.

"The aeronautical and space activities of the United States shall be conducted so as to contribute . . . to the expansion of human knowledge of phenomena in the atmosphere and space. The Administration shall provide for the widest practicable and appropriate dissemination of information concerning its activities and the results thereof."

—NATIONAL AERONAUTICS AND SPACE ACT OF 1958

NASA SCIENTIFIC AND TECHNICAL PUBLICATIONS

TECHNICAL REPORTS: Scientific and technical information considered important, complete, and a lasting contribution to existing knowledge.

TECHNICAL NOTES: Information less broad in scope but nevertheless of importance as a contribution to existing knowledge.

TECHNICAL MEMORANDUMS: Information receiving limited distribution because of preliminary data, security classification, or other reasons.

CONTRACTOR REPORTS: Technical information generated in connection with a NASA contract or grant and released under NASA auspices.

TECHNICAL TRANSLATIONS: Information published in a foreign language considered to merit NASA distribution in English.

TECHNICAL REPRINTS: Information derived from NASA activities and initially published in the form of journal articles.

SPECIAL PUBLICATIONS: Information derived from or of value to NASA activities but not necessarily reporting the results of individual NASA-programmed scientific efforts. Publications include conference proceedings, monographs, data compilations, handbooks, sourcebooks, and special bibliographies.

Details on the availability of these publications may be obtained from:

SCIENTIFIC AND TECHNICAL INFORMATION DIVISION

NATIONAL AERONAUTICS AND SPACE ADMINISTRATION

Washington, D.C. 20546